Failure Analysis of Composite Plates Subjected to Localized Loadings via a Unified Formulation

G. Giunta[1]; A. Catapano[2]; S. Belouettar[3]; P. Vannucci[4]; and E. Carrera[5]

Abstract: A failure analysis of composite plates accounting for localized loadings is presented in this work. A unified formulation is adopted to derive classical, higher order, layerwise, and mixed theories. A closed form, Navier-type solution is assumed. Simply supported, cross-ply laminates are investigated. Plates are subjected to a stepwise loading, an off-centric localized one and a localized moment. First-ply failure loading and index are obtained via several failure criteria. The influence of the side-to-thickness ratio is accounted for investigating thin and very thick plates. Symmetric and asymmetric stacking sequences are investigated. The accuracy of the proposed theories is assessed. On the basis of the obtained results, it can be concluded that higher order models are required for a correct failure analysis in which the three-dimensional stress state attributable to the localized loadings is accurately described. **DOI: 10.1061/(ASCE)EM.1943-7889.0000358.**

CE Database subject headings: Composite materials; Plates; Failures; Load factors.

Author keywords: Composite materials; Plate theories; Failure analysis; Localized loadings.

Introduction

Applications of composite materials to primary and secondary loading carrying structures have more and more increased over the last decades because of their attractive properties in strength, stiffness, and low weight. However, they present a nature more complex than classical materials do attributable to a wider number of parameters (such as anisotropy, geometry, material of the fibers, and matrix and stacking sequence) that govern their behavior. A correct design also, calls for an accurate and effective prediction of displacement and stress field. Highly accurate mechanical models are, therefore, required to effectively describe the mechanics of composite structures and their failure. As far as composites' failure models are concerned, several failure criteria have been formulated in the last decades [see Sih and Skudra (1985) and Soni (1983)]. The drawbacks and benefits of many of them have been investigated in the world wide failure exercise organized by Hinton and Soden (1998). A comparison is addressed in Soden et al. (1998). In addition to the classical failure criteria such as maximum stress, see Reddy (2004), Tsai and Wu (1971), Tsai and Hill (see Hill 1948), Hoffman (1967); Hashin (1980), LaRC04 (Pinho et al. 2005), and Puck (1996) and Puck and Schürmann's (1998, 2002) criteria are also notable. Basu et al. (2006a, 2006b, 2007) proposed a progressive damage model accounting for compressive fiber failure and kink bending. The writers showed that the concept of a fixed compressive strength is not appropriate and a nonlinear constitutive model, at least in the transverse direction, should be adopted. A literature review addressing the failure analysis of composite plates and shells can be found in Spottswood and Palazotto (2001). To the best of the writers' knowledge, Turvey (1980a) was the first to investigate the failure of composite plates. Reddy and Pandey (1987) adopted the finite-element method to study the first-ply and the post first-ply failure of several laminates in terms of failure loadings and locations. The first-order shear deformation theory by Reissner (1945) and Mindlin (1951) was assumed. Kam and Jan (1995) proposed a finite element based on a linear layerwise model of the displacement field. Several failure criteria, such as maximum stress/strain, Tsai-Wu's, Tsai-Hill's, and Hoffman's, were adopted. Numerical results were validated toward experimental data. Nonlinear effects via the Von Karman-Mindlin theory were accounted for by Kam et al. (1996). Experimental investigations were also carried out. Both geometric and material nonlinearities were assumed by Padhi et al. (1997) for studying the first-ply failure, the progression of damage, and the ultimate collapse of composite plates. First-ply and ultimate failure loading were determined experimentally by Kelly and Hallstrom (2005) in the case of composite laminates subjected to localized transverse loadings. Mohite and Upadhyay (2006) investigated the failure of composite plates under localized loadings using Tsai-Wu's criterion. A layerwise finite element was formulated by Onkar et al. (2007) for the determination of the stochastic first-ply failure loading via Tsai-Wu's and Hoffman's criteria. Huang (2007) carried out a failure analysis using a nonlinear material constitutive law based on the Bridging Model by Huang (2001). Akhras and Li (2007) performed a failure analysis using the spline finite strip method (SFSM) for thick plates and Lee's (1982) failure criterion. SFSM was also used by Zahari and El-Zafrany (2009) for a nonlinear analysis of composite laminated stiffened plates to account for finite displacements attributable to damage.

[1]Centre de Recherche Public Henri Tudor, 29, Av. J. F. Kennedy, L-1855 Luxembourg-Kirchberg, Luxembourg (corresponding author). E-mail: gaetano.giunta@tudor.lu

[2]Institut Jean Le Rond d'Alembert, UMR7190 CNRS Univ. Paris06, 4, Place Jussieu, 75252 Paris, France and Centre de Recherche Public Henri Tudor, 29, Av. J. F. Kennedy, L-1855 Luxembourg-Kirchberg, Luxembourg.

[3]Centre de Recherche Public Henri Tudor, 29, Av. J. F. Kennedy, L-1855 Luxembourg-Kirchberg, Luxembourg.

[4]Universite Versailles St. Quentin, 45, Av. des Etats-Unis, 78035 Versailles Cedex, France and Institut Jean Le Rond d'Alembert, UMR7190 CNRS Univ. Paris06, 4, Place Jussieu, 75252 Paris, France.

[5]Dept. of Aeronautic and Space Engineering, Politecnico di Torino, 24, c.so Duca degli Abruzzi, 10129 Turin, Italy.

Note. This manuscript was submitted on September 20, 2010; approved on November 21, 2011; published online on November 23, 2011. Discussion period open until October 1, 2012; separate discussions must be submitted for individual papers. This paper is part of the ***Journal of Engineering Mechanics***, Vol. 138, No. 5, May 1, 2012. ©ASCE, ISSN 0733-9399/2012/5-458–467/$25.00.

Zhang et al. (2008) proposed a triangular stiffened element and applied it to the progressive failure analysis of grid stiffened composite plates and shells. The modified Hashin's criterion as in Chang et al. (1991) was adopted. Delamination was accounted for via Chai and Gadke's (1999) criterion. The present work presents a first-ply failure analysis of composite plates subjected to localized loadings. Carrera's unified formulation (CUF) (2003) is used to derive several two-dimensional models. CUF is a systematic approach based on a formal compact notation that allows formulating a large variety of two-dimensional higher order theories via the principle of virtual displacement (PVD) or reissner's mixed variational theorem (RMVT) [see Reissner (1986)], adopting an equivalent single layer (ESL) approach or a layerwise (LW) one. Classical theories can be obtained as particular cases. A Navier-type closed form solution is assumed. Simply supported, cross-ply laminates are, therefore, investigated. Failure is described in terms of first-ply failure loading, location, and failure index. Maximum stress, Tsai-Wu's, Hoffman's, and Hashin's failure criteria are considered. The writers are aware that, as experimentally shown by Kam (1996), a nonlinear load-deflection relation might be present even before the occurrence of first-ply failure. A linear elastic behavior, however, is assumed. Plates are considered to undergo centric and off-centric localized loadings and moments. The influence of the side-to-thickness ratio is accounted for. Thin and very thick plates are investigated. Several staking sequences (symmetric and unsymmetric laminates) are considered. The accuracy of the proposed theories is assessed toward Pagano's (1970) three-dimensional exact solution. With respect to the previous work by Carrera and Giunta (2009), this paper focuses on the prediction of the first-ply failure attributable to localized loadings. To the best of the writers' knowledge, only few closed form, analytical solutions exist in literature. The present results might, therefore, represent a valid benchmark. Attention is also paid to the investigation of the role of the proposed CUF models for the stress analysis in conjunction with the classical stress-based failure criteria of composite structures aiming at demonstrating that higher-order models are required for a correct failure analysis in which a three-dimensional stress state is present.

Overview of the Considered Plate Theories

Fig. 1 presents plate's geometry, and reference system are shown. x, y, and z are the reference system axes such that: $0 \le x \le a$, $0 \le y \le b$ and $-h/2 \le z \le h/2$. The through-the-thickness direction is z and $\Omega = [(x, y, z): z = 0]$ is the reference plane of the plate. The components of the displacement vector along the x-, y, and z-axis are u_x, u_y, and u_z, respectively. N_l represents the total number of layers, k counts the laminae, and h_k stands for a k-layer thickness. A vast variety of two-dimensional theories can be formulated on the basis of different kinematic assumptions.

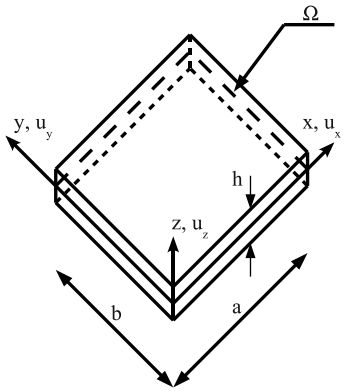

Fig. 1. Plate geometry and reference system

Classical Theories

Classical theories were conceived in the last two centuries to model the global membrane-bending mechanics.

Classical Lamination Theory

Classical lamination theory (CLT) is based on Cauchy, Poisson, and Kirchhoff's kinematic assumptions:

$$u_q(x, y, z) = u_{q0}(x, y) - z\frac{\partial u_{z0}}{\partial q} \quad \text{with } q = x, y$$
$$u_z(x, y, z) = u_{z0}(x, y) \tag{1}$$

They postulate that the normals to the reference surface Ω remain normal, straight, and unstrained after deformation. Displacement components in correspondence to the reference plane are denoted via the subscript. CLT does not account for shear and normal transverse deformations. In this paper, shear and normal out-of-plane stress components are obtained a posteriori upon integration of the indefinite equilibrium equations.

First-Order Shear Deformation Theory

Reissner and Mindlin postulated a kinematic field that accounts for constant through-the-thickness transverse shear stress and strain components:

$$u_q(x, y, z) = u_{q0}(x, y) + zu_{q1}(x, y) \quad \text{with } q = x, y$$
$$u_z(x, y, z) = u_{z0}(x, y) \tag{2}$$

The model based on these kinematic assumptions is named first-order shear deformation theory (FSDT). The normal deformation is neglected. In this paper, more accurate values of the out-of-plane shear stresses are obtained via integration of the indefinite equilibrium equations.

Higher-Order Theories

Refinements of CLT and FSDT can be introduced by including higher-order terms in the kinematic assumptions in Eqs. (2):

$$u_q(x, y, z) = u_{q0}(x, y) + z^r u_{qr}(x, y) \quad \text{with}$$
$$q = x, y, z;\ r = 1, 2, \ldots, N \tag{3}$$

The summation convention for the repeated indices has been adopted. Kinematic model in Eq. (3) accounts for both shear and normal transverse deformation. N is the order of expansion. It is supposed to be as high as four. These theories are addressed as EDN. Letter denotes that the kinematic is based on the ESL approach, indicates that displacements are assumed as unknowns, and represents the through-the-thickness approximation order.

Layerwise Theories

Multilayered plates' mechanics can be modeled by means of kinematic assumptions that are independent in each layer. According to Reddy (2004), this approach is stated as layerwise (LW). MacLaurin's expansion along the thickness, as for ESL models, is no longer convenient in this case. Displacements interlaminar congruency can be imposed more conveniently assuming interface values as unknown variables:

$$u_q^k = F_t u_{qt}^k + F_b u_{qb}^k + F_r u_{qr}^k, \quad \text{with}$$
$$q = x, y, z;\ r = 2, 3, \ldots, N;\ k = 1, 2, \ldots, N_l \tag{4}$$

J. Eng. Mech. 2012.138:458-467.

Subscripts t and b denote values related to a k-layer top and bottom surface. Thickness functions F_t, F_b, and F_r depend on a local, through-the-thickness coordinate ζ_k:

$$F_t = \frac{P_0 + P_1}{2}, \qquad F_b = \frac{P_0 - P_1}{2}, \qquad F_r = P_r - P_{r-2}, \qquad r = 2, 3, .., N \tag{5}$$

where $P_j = P_j(\zeta_k)$ is a j-order Legendre's polynomial function. The first four Legendre's polynomials are:

$$P_0 = 1, \qquad P_1 = \zeta_k, \qquad P_2 = \frac{3\zeta_k^2 - 1}{2}, \qquad P_3 = \frac{5\zeta_k^3}{2} - \frac{3\zeta_k}{2}, \qquad P_4 = \frac{35\zeta_k^4}{8} - \frac{15\zeta_k^2}{4} + \frac{3}{8} \tag{6}$$

The following properties hold:

$$\zeta_k = \begin{cases} 1: & F_t = 1,\ F_b = 0,\ F_r = 0 \\ -1: & F_t = 0,\ F_b = 1,\ F_r = 0 \end{cases} \tag{7}$$

Interlaminar compatibility of displacement can be easily imposed:

$$u_{qt}^k = u_{qb}^{(k+1)} \quad \text{with } q = x, y, z;\ k = 1, 2, \ldots, N_l - 1 \tag{8}$$

The acronym for these theories is LDN, where L stands for a LW approach.

Mixed Theories

The kinematics described previously do not ensure interlaminar continuity of shear and normal out-of-plane stresses at the interface between two adjacent layers. It can be fulfilled a priori via Reissner's mixed variational theorem (RMVT) [see Reissner (1986)]. Within RMVT framework, shear and normal transverse stresses are assumed as primary variables together with displacements. In a LW case, the following model is used to approximate the shear and normal out-of-plane stresses:

$$\sigma_{qz}^k = F_t \sigma_{qzt}^k + F_b \sigma_{qzb}^k + F_r \sigma_{qzr}^k, \quad \text{with } q = x, y, z;\ r = 2, 3, \ldots, N;\ k = 1, 2, \ldots, N_l \tag{9}$$

Interlaminar continuity is imposed in a straightforward manner:

$$\sigma_{qzt}^k = \sigma_{qzb}^{(k+1)} \quad \text{with } q = x, y, z;\ k = 1, 2, \ldots, N_l - 1 \tag{10}$$

A model of this group is denoted as LMN, where = mixed models based on RMVT.

Carrera's Unified Formulation

The considered theories are all unified considering that CLT and FSDT are a particular case of higher order ESL models. These latter can be regarded as a peculiar case of LW models in which the number of layers is equal to the unit and the polynomial approximation is obtained via the classical base $\{z^r : r = 0, 1, \ldots, N\}$. Eqs. (1)–(4) can be unified into the following compact vectorial notation:

$$\mathbf{u}^k = F_t \mathbf{u}_t^k + F_b \mathbf{u}_b^k + F_2 \mathbf{u}_2^k + \ldots + F_N \mathbf{u}_N^k = F_\tau \mathbf{u}_\tau^k \quad \tau = t, b, r;\ r = 2, 3, \ldots, N;$$
$$\boldsymbol{\sigma}^k = F_t \boldsymbol{\sigma}_t^k + F_b \boldsymbol{\sigma}_b^k + F_2 \boldsymbol{\sigma}_2^k + \ldots + F_N \boldsymbol{\sigma}_N^k = F_\tau\, \boldsymbol{\sigma}_\tau^k \quad k = 1, 2, \ldots, N_l \tag{11}$$

$$\mathbf{u}^k = \begin{Bmatrix} u_x^k \\ u_y^k \\ u_z^k \end{Bmatrix}, \qquad \boldsymbol{\sigma}^k = \begin{Bmatrix} \boldsymbol{\sigma}_{xz}^k \\ \boldsymbol{\sigma}_{yz}^k \\ \boldsymbol{\sigma}_{zz}^k \end{Bmatrix} \tag{12}$$

The derivation of the governing equations according to the chosen variational statement becomes general, regardless of the approximation approach (ESL or LW), the polynomial functions, or the approximation order.

Governing Equations

For the sake of brevity, governing equations and related mechanical and geometrical boundary conditions are addressed assuming the PVD only. Their derivation from RMVT is straightforward and it can be found in Carrera (2003). Considering a generic pressure loading $\mathbf{p}^{kT} = \{p_x^k, p_y^k, p_z^k\}$ acting on the top, Σ_k^t, and the bottom, Σ_k^b, of each lamina, the variational statement based on the PVD is

$$N_l \sum_{k=1} \int_{\Omega_k} \int_{h_k} \delta \boldsymbol{\epsilon}_p^{kT} \boldsymbol{\sigma}_p^k + \delta \boldsymbol{\epsilon}_n^{kT} \boldsymbol{\sigma}_n^k dz_k d\Omega_k = N_l \sum_{k=1} \int_{\Sigma_k^b \bigcup \Sigma_k^t} \delta \mathbf{u}^{kT} \mathbf{p}^k d\Omega_k \tag{13}$$

in which

$$\boldsymbol{\epsilon}_p = \begin{Bmatrix} \boldsymbol{\epsilon}_{xx} \\ \boldsymbol{\epsilon}_{yy} \\ \boldsymbol{\epsilon}_{xy} \end{Bmatrix}, \qquad \boldsymbol{\epsilon}_n = \begin{Bmatrix} \boldsymbol{\epsilon}_{xz} \\ \boldsymbol{\epsilon}_{yz} \\ \boldsymbol{\epsilon}_{zz} \end{Bmatrix}; \qquad \boldsymbol{\sigma}_p = \begin{Bmatrix} \boldsymbol{\sigma}_{xx} \\ \boldsymbol{\sigma}_{yy} \\ \boldsymbol{\sigma}_{xy} \end{Bmatrix}, \qquad \sigma_n = \begin{Bmatrix} \boldsymbol{\sigma}_{xz} \\ \boldsymbol{\sigma}_{yz} \\ \boldsymbol{\sigma}_{zz} \end{Bmatrix} \tag{14}$$

are the in- and out-of-plane strains and stresses in the structure reference system [see Fig. 1]. Voigt's notation is assumed to address stresses in the material reference system. Stresses and strains of a k-layer are related via the well-known Hooke's law:

$$\boldsymbol{\sigma}_p^k = \mathbf{C}_{pp}^k \boldsymbol{\epsilon}_p^k + \mathbf{C}_{pn}^k \qquad \boldsymbol{\sigma}_n^k = \mathbf{C}_{np}^k \boldsymbol{\epsilon}_p^k + \mathbf{C}_{nn}^k \boldsymbol{\epsilon}_n^k \tag{15}$$

in which $[\mathbf{C}_{ij}^k : i, j = pn]$ are the material stiffnesses. Displacements-strains relations are

$$\boldsymbol{\epsilon}_p^k = \mathbf{D}_p \mathbf{u}^k \qquad \boldsymbol{\epsilon}_n^k = \mathbf{D}_{n\Omega} \mathbf{u}^k + \mathbf{D}_{nz} \mathbf{u}^k \tag{16}$$

$\mathbf{D}_p$, $\mathbf{D}_{n\Omega}$, and $\mathbf{D}_{nz}$ are matrices of differential operators defined as follows:

$$\mathbf{D}_p = \begin{bmatrix} \frac{\partial}{\partial x} & 0 & 0 \\ 0 & \frac{\partial}{\partial y} & 0 \\ \frac{\partial}{\partial y} & \frac{\partial}{\partial x} & 0 \end{bmatrix}, \qquad \mathbf{D}_{n\Omega} = \begin{bmatrix} 0 & 0 & \frac{\partial}{\partial x} \\ 0 & 0 & \frac{\partial}{\partial y} \\ 0 & 0 & 0 \end{bmatrix},$$
$$\mathbf{D}_{nz} = \begin{bmatrix} \frac{\partial}{\partial z} & 0 & 0 \\ 0 & \frac{\partial}{\partial z} & 0 \\ 0 & 0 & \frac{\partial}{\partial z} \end{bmatrix} \tag{17}$$

Replacing Eqs. (15) and (16) and the postulated, unified displacement field $\mathbf{u} = F_\tau \mathbf{u}_\tau$ into Eq. (13) and after some algebraic manipulations and application of Gauss-Green's theorem, the variational statement becomes

$$\sum_{k=1}^{N_l}\int_{\Omega_k}\delta\mathbf{u}_\tau^{kT}\int_{h_k}\{-F_\tau\mathbf{D}_p^T[\mathbf{C}_{pp}^k F_s\mathbf{D}_p+\mathbf{C}_{pn}^k(F_s\mathbf{D}_{n\Omega}+F_{s,z})]$$
$$+(-F_\tau\mathbf{D}_{n\Omega}^T+F_{\tau,z})[\mathbf{C}_{np}^k F_s\mathbf{D}_p+\mathbf{C}_{nn}^k(F_s\mathbf{D}_{n\Omega}+F_{s,z})]\}dz_k\mathbf{u}_s^k d\Omega_k$$
$$+\sum_{k=1}^{N_l}\int_{\Gamma_k}\delta\mathbf{u}_\tau^{kT}\int_{h_k}\{F_\tau\mathbf{I}_p^T[\mathbf{C}_{pp}^k F_s\mathbf{D}_p+\mathbf{C}_{pn}^k(F_s\mathbf{D}_{n\Omega}+F_{s,z})]$$
$$+F_\tau\mathbf{I}_{n\Omega}^T[\mathbf{C}_{np}^k F_s\mathbf{D}_p+\mathbf{C}_{nn}^k(F_s\mathbf{D}_{n\Omega}+F_{s,z})]\}dz_k\mathbf{u}_s^k d\Omega_k$$
$$=\sum_{k=1}^{N_l}\int_{\Sigma_k^b\bigcup\Sigma_k^t}\delta\mathbf{u}_\tau^{kT}\mathbf{p}_\tau^k d\Omega_k \tag{18}$$

$\mathbf{p}_\tau^k$ = a variationally consistent load vector coming from the applied loadings $\mathbf{p}^k$. Eq. (18) yields the governing equations and the boundary conditions through an appropriate choice of the virtual displacements:

$$\begin{aligned}&\mathbf{K}_d^{k\tau s}\mathbf{u}_s^k=\mathbf{p}_\tau^k \qquad \mathbf{u}_\tau^k=\overline{\mathbf{u}}_\tau^k \quad (x,y,z)\in\Gamma_k^g\\&\mathbf{\Pi}_d^{k\tau s}\mathbf{u}_s^k=\mathbf{\Pi}_d^{k\tau s}\overline{\mathbf{u}}_s^k \quad (x,y,z)\in\Gamma_k^m\end{aligned} \tag{19}$$

being the k-layer geometrical boundary conditions ($\overline{\mathbf{u}}_\tau^k$) applied on Γ_k^g and the mechanical ones ($\mathbf{\Pi}_d^{k\tau s}\overline{\mathbf{u}}_s^k$) on Γ_k^m. Differential matrices $\mathbf{K}_d^{k\tau s}$ and $\mathbf{\Pi}_d^{k\tau s}$ are:

$$\mathbf{K}_d^{k\tau s}=\int_{h_k}\{-F_\tau\mathbf{D}_p^T[\mathbf{C}_{pp}^k F_s\mathbf{D}_p+\mathbf{C}_{pn}^k(F_s\mathbf{D}_{n\Omega}+F_{s,z})]$$
$$+(-F_\tau\mathbf{D}_{n\Omega}^T+F_{\tau,z})[\mathbf{C}_{np}^k F_s\mathbf{D}_p+\mathbf{C}_{nn}^k(F_s\mathbf{D}_{n\Omega}+F_{s,z})]\}dz_k \tag{20}$$

$$\mathbf{\Pi}_d^{k\tau s}=\int_{h_k}\{F_\tau\mathbf{I}_p^T[\mathbf{C}_{pp}^k F_s\mathbf{D}_p+\mathbf{C}_{pn}^k(F_s\mathbf{D}_{n\Omega}+F_{s,z})]$$
$$+F_\tau\mathbf{I}_{n\Omega}^T[\mathbf{C}_{np}^k F_s\mathbf{D}_p+\mathbf{C}_{nn}^k(F_s\mathbf{D}_{n\Omega}+F_{s,z})]\}dz_k \tag{21}$$

A Navier's solution of Eq. (19) can be obtained by assuming the following harmonic form for the applied loadings and unknown displacements:

$$\begin{aligned}(u_x^k,p_{xz}^k)&=\sum_{m=1}^{\bar m}\sum_{n=1}^{\bar n}[U_x^k(z),\ P_{xz}^k(z)]\cos\left(\frac{m\pi}{a}x\right)\sin\left(\frac{n\pi}{b}y\right)\\(u_y^k,\ p_{yz}^k)&=\sum_{m=1}^{\bar m}\sum_{n=1}^{\bar n}[U_y^k(z),\ P_{yz}^k(z)]\sin\left(\frac{m\pi}{a}x\right)\cos\left(\frac{n\pi}{b}y\right)\\(u_z^k,p_{zz}^k)&=\sum_{m=1}^{\bar m}\sum_{n=1}^{\bar n}[U_z^k(z),\ P_{zz}^k(z)]\sin\left(\frac{m\pi}{a}x\right)\sin\left(\frac{n\pi}{b}y\right)\end{aligned} \tag{22}$$

Results and Discussion

First-ply failure load value, damage location, and failure indices are computed for simply supported cross-ply laminates according to maximum stress, Tsai-Wu's, Hoffman's, and Hashin's criteria. These criteria are reported in the Appendix to ease the analysis of the requested polynomial order and the role of the different stress components. Results are assessed toward Pagano's three-dimensional solution. The through-the-thickness variation of the failure index in which the loading amplitude is equal to the exact minimum failure loading is also presented. Unless differently stated, a symmetric [0/90/0] configuration is considered. Stacking sequence starts from plate top. Ply angles are measured toward x-axis. The plies are all made of T300/5208 graphite/epoxy as in Pandey and Reddy (1987). Mechanical properties lamina principal coordinates (1,2,3) are: $E_1 = 132.410^3$ MPa, $E_2 = E_3 = 10.710^3$ MPa, $G_{12} = G_{13} = 5.6510^3$ MPa, $G_{23} = 3.3810^3$ MPa, $\nu_{12} = \nu_{13} = 0.24$, and $\nu_{23} = 0.49$. Material strength parameters are: $X_t = 1513.4$ MPa, $X_c = 1696$ MPa, $Y_t = Z_t = 43.8$ MPa, $Y_c = Z_c = 164$ MPa, $S = T = 86.9$ MPa, and $R = 67.6$ MPa. The plies all have the same thickness. Plate sides are of equal length: $a = b = 0.1$ m. The side-to-thickness ratio (a/h) is considered as an analysis parameter. It can be as high as 100 and as low as 5; thin and thick plates are, therefore, investigated. Stepwise, off-centric localized loadings and a localized moment are considered. Loadings are applied on the plate's top and directed along the positive direction of the z-axis. The number of harmonic terms, $\overline{m}$ and $\overline{n}$, in the Fourier series approximation of the loadings is such to ensure a convergence of the first four significant digits of the failure loading. Failure locations are obtained as a consequence of the convergence of the failure loading value. Results have shown that failure occurs in an area around the failure point whose dimension depends on the stress gradients present there. The value of the failure loading in the failure area is very close to the one of the failure point. A failure location in terms of points is used for comparing the results.

Stepwise Localized Loading

The stepwise loading is applied such that $0 \le x \le a$ and $b/3 \le y \le 2b/3$ [see Fig. 2]. $\overline{m}$ and $\overline{n}$ in Eqs. (22) are equal to 21. Minimum failure loading and failure location computed via Pagano's three-dimensional solution are reported in Table 1. Failure occurs at plate center for a/h as low as 50. For thick and very thick plates, the failure criteria yield different in-plane failure positions. In the case of $a/h = 5$, according to maximum stress criterion failure occurs at point $(\frac{1}{2}, \frac{1}{2} \pm \frac{1}{48}, \frac{1}{2})$, whereas for all the other criteria it is at point $(\frac{1}{2}, \frac{1}{2} \pm \frac{1}{24}, \frac{1}{2})$. The difference between the maximum and the minimum failure loading value increases when a/h decreases. For a/h as low as 50, the difference is approximately 6%, whereas it is approximately 26% for very thick plates. The differences in value and

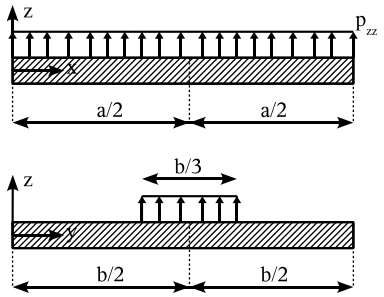

Fig. 2. Stepwise loading

Table 1. Minimum First-Ply Failure Loading and Failure Location via Pagano's Three-Dimensional Solution, Stepwise Loading

a/h [MPa]	100×10^{-2}	50×10^{-1}	10×1	5×10
Maximum stress	7.546	3.001	6.374	1.795
	$(\frac{1}{2}, \frac{1}{2}, \frac{1}{2})^a$	$(\frac{1}{2}, \frac{1}{2}, \frac{1}{2})$	$(\frac{1}{2}, \frac{1}{2}, \frac{1}{2})$	$(\frac{1}{2}, \frac{1}{2} \pm \frac{1}{48}, \frac{1}{2})$
Tsai-Wu	7.802	3.098	6.250	1.532
	$(\frac{1}{2}, \frac{1}{2}, \frac{1}{2})^a$	$(\frac{1}{2}, \frac{1}{2}, \frac{1}{2})$	$(\frac{1}{2}, \frac{1}{2}, \frac{1}{2})$	$(\frac{1}{2}, \frac{1}{2} \pm \frac{1}{24}, \frac{1}{2})$
Hoffman	7.253	2.884	6.009	1.569
	$(\frac{1}{2}, \frac{1}{2}, \frac{1}{2})^a$	$(\frac{1}{2}, \frac{1}{2}, \frac{1}{2})$	$(\frac{1}{2}, \frac{1}{2}, \frac{1}{2})$	$(\frac{1}{2}, \frac{1}{2} \pm \frac{1}{24}, \frac{1}{2})$
Hashin	7.535	2.985	5.689	1.314
	$(\frac{1}{2}, \frac{1}{2}, \frac{1}{2})^a$	$(\frac{1}{2}, \frac{1}{2}, \frac{1}{2})$	$(\frac{1}{2}, \frac{1}{2} \pm \frac{1}{48}, \frac{1}{2})$	$(\frac{1}{2}, \frac{1}{2} \pm \frac{1}{24}, \frac{1}{2})$

[a]Failure location (x/a, y/b, z/h).

J. Eng. Mech. 2012.138:458-467.

Table 2. Minimum First-Ply Failure Loading via Hoffman's Criterion, Stepwise Loading

a/h [MPa]	100×10^{-2}	50×10^{-1}	10×1	5×10
Pagano	7.253	2.884	6.009	1.569
CLT, FSDT	7.262, 1.00[a]	2.897, 1.00	6.646, 1.11	2.019, —
ED2	7.251, 1.00	2.888, 1.00	6.300, 1.05	1.746, —
ED3	7.245, 1.00	2.879, 1.00	5.927, 0.99	1.512, —
ED4	7.271, 1.00	2.891, 1.00	6.056, 1.01	1.585, 1.01
LD2	7.253, 1.00	2.883, 1.00	5.995, 1.00	1.560, 0.99
LD3	7.253, 1.00	2.884, 1.00	6.006, 1.00	1.570, 1.00
LD4	7.253, 1.00	2.884, 1.00	6.009, 1.00	1.569, 1.00
LM2	7.253, 1.00	2.884, 1.00	6.010, 1.00	1.575, 1.00
LM3	7.253, 1.00	2.884, 1.00	6.010, 1.00	1.572, 1.00
LM4	7.253, 1.00	2.884, 1.00	6.009, 1.00	1.569, 1.00

[a]Two- and three-dimensional failure loading ratio in the case of coincident failure location.

Table 3. Minimum First-Ply Failure Loading via the Hashin's Criterion, Stepwise Loading

a/h [MPa]	100×10^{-2}	50×10^{-1}	10×1	5×10
Pagano	7.535	2.985	5.689	1.314
CLT, FSDT	7.545, 1.00[a]	3.000, 1.01	6.274, —	1.646, —
ED2	7.533, 1.00	2.989, 1.00	5.956, —	1.445, —
ED3	7.527, 1.00	2.981, 1.00	5.622, —	1.276, —
ED4	7.555, 1.00	2.993, 1.00	5.735, 1.01	1.327, 1.01
LD2	7.535, 1.00	2.985, 1.00	5.677, 1.00	1.309, 1.00
LD3	7.535, 1.00	2.985, 1.00	5.686, 1.00	1.314, 1.00
LD4	7.535, 1.00	2.985, 1.00	5.689, 1.00	1.314, 1.00
LM2	7.535, 1.00	2.985, 1.00	5.688, 1.00	1.319, 1.00
LM3	7.535, 1.00	2.985, 1.00	5.691, 1.00	1.314, 1.00
LM4	7.535, 1.00	2.985, 1.00	5.689, 1.00	1.314, 1.00

[a]Two- and three-dimensional failure loading ratio in the case of coincident failure location.

position are attributable to the manner each criterion accounts for the out-of-plane stress components. The criteria yield all as through-the-thickness failure position the plate top. Failure occurs in the matrix being the ratio between σ_2 and the corresponding strength parameter the relevant term in all of the failure criteria. For a/h as low as 50, Hoffman's criterion is the most conservative one, whereas Tsai-Wu's criterion yields the highest value of the failure loading. In the case of a/h as high as 10, maximum stress criterion yields the highest failure loading and Hashin's criterion the minimum one. As far as two-dimensional models are concerned, only Hoffman's and Hashin's criteria are considered. Maximum stress and Tsai-Wu's criteria yield similar results to Hoffman's and Hashin's criteria, respectively. Tables 2 and 3 present the minimum failure loading and the ratio between the two- and three-dimensional failure loadings. This latter one is computed in the case of coincident failure location only. Classical theories yield accurate results for a/h as low as 50. In the case of relatively thick plates, CLT and FSDT overestimates the minimum failure loading by approximately 11% or they do not predict the correct failure location. ED2 and ED4 models represent an improvement of classical theories, being the error for $a/h = 10$ and Hoffman's criterion approximately 5% and 1%, respectively. Second-order LW models match Pagano's solution for any value of the side-to-thickness ratio, with an error of approximately 1% at worst. Fig. 3 present the failure index along the through-the-thickness coordinate at failure in-plane point via maximum stress and Hashin's criteria. Maximum stress criterion exhibits a linear variation because the problem is governed by bending. The failure index is proportional to the through-the-thickness variation of σ_2. Hashin's criterion presents a parabolic variation. Two different equations govern this variation according to the sign of the normal stresses. The main contribution to failure is attributable to σ_2. Results obtained via CLT match the exact three-dimensional solution. The failure index for thick plates is presented in Figs. 4. Hoffman's and Hashin's criteria are considered. The contribution to failure is attributable to σ_2 stress component as in the case of thin plates. CLT and first-order ESL model underestimate the failure index. LM1 model overestimates it. ED4 and second-order LW models match Pagano's exact solution.

Off-Centric Localized Loading

A stepwise off-centric localized loading is considered. Loading application area is square, centered at point $(a/4, b/4)$ and with a length equal to $a/10$ [see Fig. 5]. $\overline{m}$ and $\overline{n}$ in Eqs. (22) are equal to 38. First-ply failure load values and locations via Pagano's solutions are presented in Table 4. In this case, the values of the failure loading are higher than that of the previous case attributable to a smaller loading application area and the proximity to the supports. In-plane failure location is the center of the loading patch $(x/a = y/b = 1/4)$ for a/h as low as 50. For any value of a/h and failure criterion, failure occurs at the plate's top. It is attributable, therefore, to normal stresses, being the main contribution provided by to σ_2. Hashin's criterion is the most conservative for a/h as high as 50. In the case of very thin plates, Hoffman's criterion is the most conservative one. Tsai-Wu's criterion (for thin plates) and

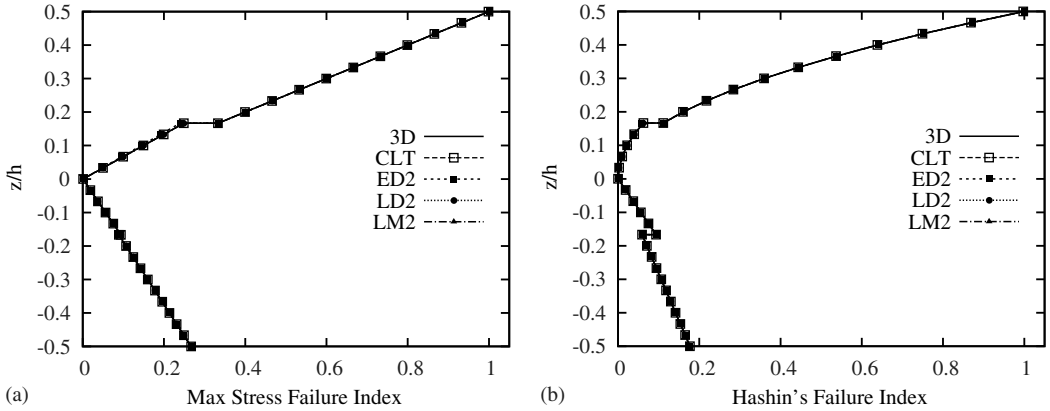

Fig. 3. Failure index via (a) maximum stress and (b) Hashin's criterion for $a/h = 100$ and stepwise loading

J. Eng. Mech. 2012.138:458-467.

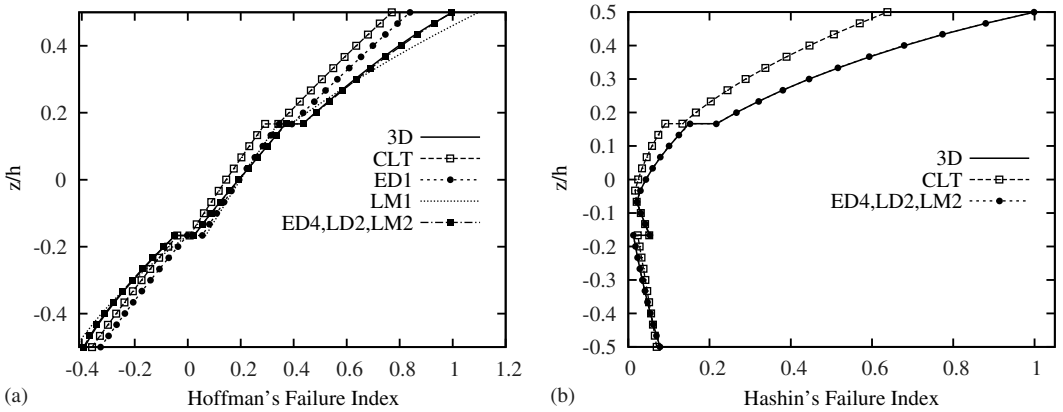

Fig. 4. Failure index via (a) Hoffman's and (b) Hashin's criterion for $a/h = 5$ and stepwise loading

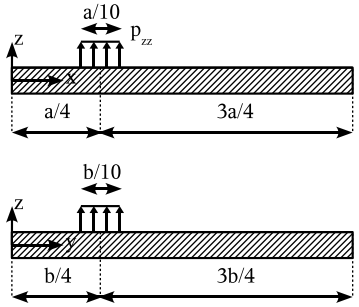

Fig. 5. Off-centric localized loading

maximum stress criterion (for thick plates) yield the highest first-ply failure loadings. Tables 5 and 6 address the failure loadings computed via CUF two-dimensional models in the case of Tsai-Wu's and Hashin's criteria, respectively. Classical models yield accurate results for thin plates as also shown in Fig. 6 where the through-the-thickness variation of Hashin's criterion for $a/h = 100$ is presented. In the case of $a/b = 50$, the error is approximately 4%. For a/h as high as 10, classical models and ED2 theory yield inaccurate results. Results obtained via a ED4 model differ from Pagaon's solution by approximately 2% and 8% for $a/h = 10$ and 5, respectively. Accurate results call for a LW approach. In particular, for Hashin's criterion a third-order approximation, at least, is required. This is attributable to the presence of a high through-the-thickness stress gradient as shown in Fig. 7. The through-the-thickness variation of Hashin's criterion for a very thick plate is there addressed.

Localized Moment

A localized moment is applied as in Fig. 8. $\overline{m}$ and $\overline{n}$ in Eqs. (22) are equal to 60. Results via Pagano's solution are reported in Table 7. For a fixed failure criterion, failure position changes versus the side-to-thickness ratio. Tsai-Wu's, Hoffman's, and Hashin's criteria yield the same failure points for a fixed value of a/h. The maximum

Table 5. Minimum First-Ply Failure Loading via Tsai-Wu's Criterion, Off-Centric Localized Loading

a/h [MPa]	100×10^{-1}	50×1	10×10	5×10
Pagano	8.500	3.200	2.103	2.463
CLT, FSDT	8.594, 1.01[a]	3.331, 1.04	2.867, 1.36	3.367, 1.37
ED2	8.529, 1.00	3.249, 1.02	2.423, 1.15	3.035, 1.23
ED3	8.477, 1.00	3.177, 0.99	2.182, 1.04	2.804,1.14
ED4	8.534, 1.00	3.218, 1.01	2.145, 1.02	2.658, 1.08
LD2	8.496, 1.00	3.196, 1.00	2.113, 1.00	2.633, 1.07
LD3	8.500, 1.00	3.200, 1.00	2.086, 0.99	2.499, 1.01
LD4	8.500, 1.00	3.200, 1.00	2.093, 1.00	2.453, 1.00
LM2	8.500, 1.00	3.201, 1.00	2.127, 1.01	2.633, 1.07
LM3	8.500, 1.00	3.200, 1.00	2.098, 1.00	2.510, 1.02
LM4	8.500, 1.00	3.200, 1.00	2.097, 1.00	2.464, 1.00

[a]Two- and three-dimensional failure loading ratio in the case of coincident failure location.

Table 6. Minimum First-Ply Failure Loading via Hashin's Criterion, Off-Centric localized Loading

a/h [MPa]	100×10^{-1}	50×1	10×10	5×10
3D	8.177	3.022	1.764	2.084
CLT, FSDT	8.266, 1.01[a]	3.141, 1.04	2.491, 1.41	3.190, —
ED2	8.205, 1.00	3.067, 1.01	2.052, 1.16	2.705, —
ED3	8.155, 1.00	3.001, 0.99	1.834, 1.03	2.431, —
ED4	8.209, 1.00	3.038, 1.01	1.803, 1.02	2.280, —
LD2	8.174, 1.00	3.018, 1.00	1.777, 1.01	2.257, —
LD3	8.177, 1.00	3.022, 1.00	1.751, 0.99	2.124, 1.02
LD4	8.177, 1.00	3.022, 1.00	1.756, 1.00	2.080, 1.00
LM2	8.177, 1.00	3.022, 1.00	1.787, 1.01	2.257, —
LM3	8.177, 1.00	3.022, 1.00	1.761, 1.00	2.134, 1.02
LM4	8.177, 1.00	3.022, 1.00	1.760, 1.00	2.083, 1.00

[a]Two- and three-dimensional failure loading ratio in the case of coincident failure location.

Table 4. Minimum First-Ply Failure Loading and Failure Location via Pagano's Three-Dimensional Solution, Off-Centric Localized Loading

a/h [MPa]	100×10^{-1}	50×1	10×10	5×10
Maximum stress	8.281 $(\frac{1}{4}, \frac{1}{4}, \frac{1}{2})$[a]	3.166 $(\frac{1}{4}, \frac{1}{4}, \frac{1}{2})$	3.202 $(\frac{11}{40}, \frac{9}{40}, \frac{1}{2})$	3.535 $(\frac{5}{18}, \frac{5}{18}, \frac{1}{2})$
Tsai-Wu	8.500 $(\frac{1}{4}, \frac{1}{4}, \frac{1}{2})$	3.200 $(\frac{1}{4}, \frac{1}{4}, \frac{1}{2})$	2.103 $\frac{11}{40}, \frac{9}{40}, \frac{1}{2}$	2.463 $(\frac{5}{18}, \frac{5}{18}, \frac{1}{2})$
Hoffman	8.026 $(\frac{1}{4}, \frac{1}{4}, \frac{1}{2})$	3.050 $(\frac{1}{4}, \frac{1}{4}, \frac{1}{2})$	2.252 $(\frac{11}{40}, \frac{9}{40}, \frac{1}{2})$	2.656 $(\frac{5}{18}, \frac{5}{18}, \frac{1}{2})$
Hashin	8.177 $(\frac{1}{4}, \frac{1}{4}, \frac{1}{2})$	3.022 $(\frac{1}{4}, \frac{1}{4}, \frac{1}{2})$	1.764 $(\frac{11}{40}, \frac{9}{40}, \frac{1}{2})$	2.084 $(\frac{5}{18}, \frac{5}{18}, \frac{1}{2})$

[a]Failure location $(x/a, y/b, z/h)$.

J. Eng. Mech. 2012.138:458-467.

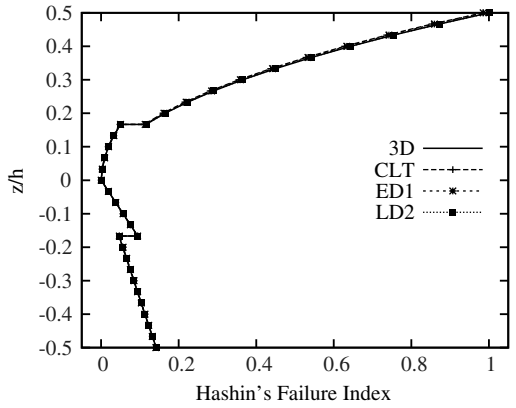

Fig. 6. Failure index via Hashin's criterion for $a/h = 100$, off-centric localized loading

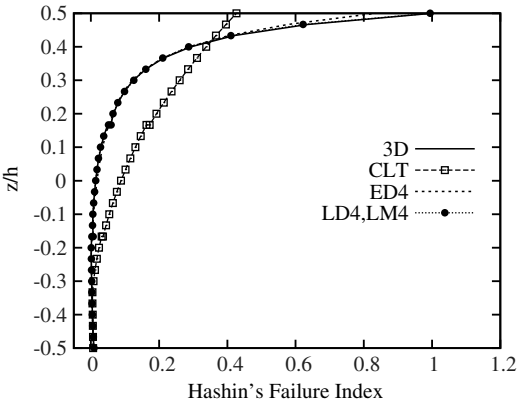

Fig. 7. Failure index via Hashin's criterion for $a/h = 5$, off-centric localized loading

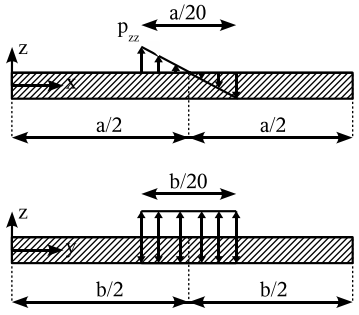

Fig. 8. Localized moment

stress criterion predicts the highest failure loading. In accordance with this criterion, the minimum failure loading is constant for a/h as high as 50. This is attributable to the fact that σ_{zz} is responsible for failure. Tables 8 and 9 present minimum first-ply failure loads computed via CUF models. Maximum stress and Hashin's criteria are considered. As far as maximum stress criterion is concerned, two-dimensional higher order models yield accurate results because out-of-plane stress components are obtained via integration of the indefinite equilibrium equations starting from the plate's top. In the case of Hashin's criterion, classical models yields inaccurate results. ESL models yield good results for a/h as low as 50. For $a/h \leq 10$, they do not predict the correct failure location. The stress field is fully three-dimensional and, therefore, difficult to be

Table 7. Minimum First-Ply Failure Loading and Failure Location via Pagano's Three-Dimensional Solution, Localized Moment

a/h [MPa]	100×10	50×10	10×10	5×10
Maximum stress	4.163	7.091	7.091	7.091
	$(\frac{21}{40}, \frac{1}{2}, \frac{1}{2})$[a]	$(\frac{41}{80}, \frac{1}{2}, \frac{1}{2})$	$(\frac{41}{80}, \frac{1}{2}, \frac{1}{2})$	$(\frac{41}{80}, \frac{1}{2}, \frac{1}{2})$
Tsai-Wu	3.701	4.931	5.514	5.520
	$(\frac{21}{40}, \frac{1}{2}, \frac{1}{2})$	$(\frac{41}{80}, \frac{1}{2}, \frac{1}{2})$	$(\frac{41}{80}, \frac{1}{2} \pm \frac{1}{80}, \frac{1}{2})$	$(\frac{41}{80}, \frac{1}{2} \pm \frac{1}{80}, \frac{1}{2})$
Hoffman	3.551	5.155	5.844	5.851
	$(\frac{21}{40}, \frac{1}{2}, \frac{1}{2})$	$(\frac{41}{80}, \frac{1}{2}, \frac{1}{2})$	$(\frac{41}{80}, \frac{1}{2} \pm \frac{1}{80}, \frac{1}{2})$	$(\frac{41}{80}, \frac{1}{2} \pm \frac{1}{80}, \frac{1}{2})$
Hashin	3.045	4.089	4.692	4.699
	$(\frac{41}{80}, \frac{1}{2}, \frac{1}{2})$	$(\frac{41}{80}, \frac{1}{2}, \frac{1}{2})$	$(\frac{41}{80}, \frac{1}{2} \pm \frac{1}{80}, \frac{1}{2})$	$(\frac{41}{80}, \frac{1}{2} \pm \frac{1}{80}, \frac{1}{2})$

[a]Failure location $(x/a, y/b, z/h)$.

Table 8. Minimum First-Ply Failure Loading via Maximum Stress Criterion, Localized Moment

a/h [MPa]	100×10	$\leq 50 \times 10$
Pagano	4.163	7.091
CLT, FSDT	4.593, —	7.091, 1.00[a]
ED2	4.478, 1.07	7.091, 1.00
ED3	4.012, 0.96	7.091, 1.00
ED4	4.175, 1.00	7.091, 1.00

[a]Two- and three-dimensional failure loading ratio in the case of coincident failure location.

Table 9. Minimum First-Ply Failure Loading via Hashin's Criterion, Localised Moment

a/h [MPa]	100×10	50×10	10×10	5×10
Pagano	3.045	4.089	4.692	4.699
CLT, FSDT	3.810, —	5.728, 1.40[a]	6.989, —	7.064, —
ED2	3.211, 1.05	4.291, 1.05	5.960, —	6.583, —
ED3	2.935, 0.96	3.935, 0.96	5.319, —	6.047, —
ED4	3.044, 1.00	4.081, 1.00	4.909, —	5.489, —
LD2	3.009, 1.00	4.049, 0.99	4.985, —	5.580, —
LD3	3.035, 1.00	4.054, 0.99	4.721, —	4.969, —
LD4	3.045, 1.00	4.085, 1.00	4.651, 0.99	4.758, —
LM2	3.037, 1.00	4.058, 0.99	4.910, —	5.433, —
LM3	3.040, 1.00	4.074, 1.00	4.763, 1.01	4.956, —
LM4	3.045, 1.00	4.086, 1.00	4.669, 1.00	4.769, —

[a]Two- and three-dimensional failure loading ratio in the case of coincident failure location.

described via two-dimensional models. In the case of Hashin's criterion, LM4 is the only model that yields good results for $a/h = 10$. For a side-to-thickness ratio equal to five, all the considered models do not predict the correct failure location. The solution can be improved increasing the approximation order or, in the case of LW models, via the assumption of mathematical interfaces.

Table 10. Minimum First-Ply Failure Loading via LM4 Theory with N_i Mathematical Interfaces at Top Layer, $a/h = 5$, Localized Moment

[MPa]	$N_i = 1$	$N_i = 2$
Tsai-Wu's	55.03, 1.00[a]	55.06, 1.00
Hoffmann's	58.61, 1.00	58.47, 1.00
Hashin's	46.99, 1.00	46.99, 1.00

[a]Two- and three-dimensional failure loading ratio in the case of coincident failure location.

J. Eng. Mech. 2012.138:458-467.

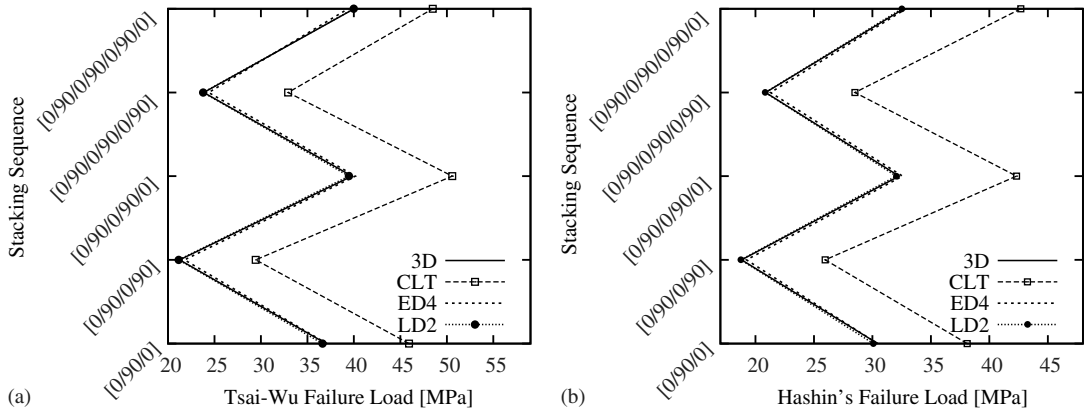

Fig. 9. Failure loading via (a) Tsai-Wu's and (b) Hashin's criterion for $a/h = 100$, localized moment

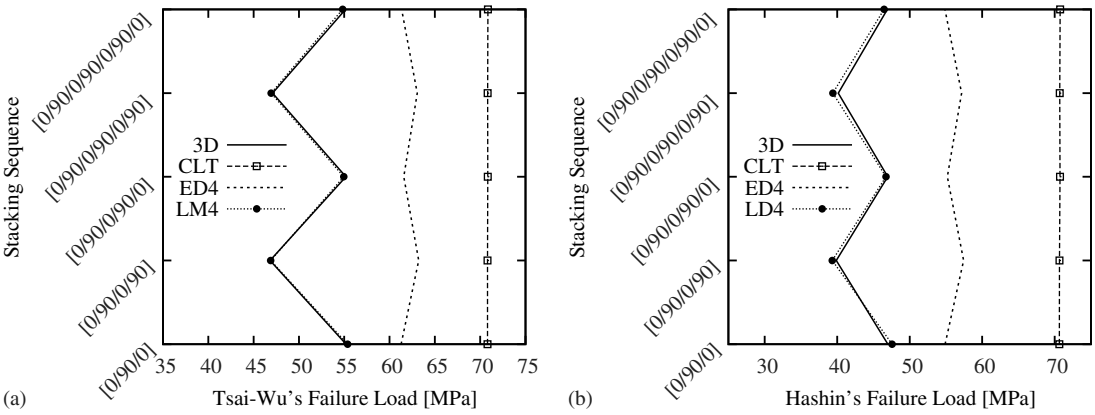

Fig. 10. Failure loading via (a) Tsai-Wu's and (b) Hashin's criterion for $a/h = 5$, localized moment

In this last case, each layer is ideally split into $N_i + 1$ sublayers, being N_i the number of mathematical interfaces. Table 10 presents the minimum first-ply failure loading computed via LM4 theory with one and two mathematical interfaces at top layer. The thickness is the same in each sublayer. Results converge to the reference exact solution. It should be underlined that for this loading case, a correct prediction of the three-dimensional stress state is required and high-order LW theories should, therefore, be adopted.

Effect of the Stacking Sequence

Analyses are carried out considering several symmetric and asymmetric staking sequences. The total thickness of each laminate is constant. Failure loading value for thin and very thick plates are reported in Figs. 9 and 10, respectively. Tsai-Wu's and Hashin's failure criteria are considered. First-ply failure loading strongly depends on the stacking sequence. In particular, the failure loading of symmetric sequences is higher than that of unsymmetric ones. Hashin's criterion is more conservative than Tsai-Wu's one for both values of a/h. As far as two-dimensional models are concerned, CLT heavily overestimates the failure loading. ED4 model yields good results only in the case of $a/h = 100$. LW theories match the exact three-dimensional solution via a second-order expansion for $a/h = 100$ and a fourth order expansion for $a/h = 5$.

Conclusions

A study of the onset of failure in composite plates subjected to localized loadings has been presented. Failure has been addressed in terms of minimum first-ply failure loadings, failure locations, and indices via maximum stress, Tsai-Wu's, Hoffman's, and Hashin's failure criteria. Thin and very thick plates have been investigated. Plate mechanics have been described via two-dimensional models formulated via Carrera's unified formulation (CUF). CUF allows obtaining a vast variety of theories from the classical ones to higher order, mixed, layerwise theories. In this manner, transverse shear and normal deformations can be accounted for. Interface equilibrium of out-of-plane stress components is ensured. Change in slope of displacements and out-of-plane stresses at the ply interface, peculiar of composite laminates, can be modeled. Governing equations have been solved via Navier's solution. Simply supported plates have been, therefore, investigated. Accuracy of CUF models has been verified through comparison with Pagano's three-dimensional exact solution. Classical models yield accurate results for a side-to-thickness ratio (a/h) as low as 50 and stepwise and off-centric localized loadings. In the case of localized moment, higher order models should be preferred even for thin plates. Higher order equivalent single layer models yield accurate results for $a/h = 50$ and 10 unless the loading condition is such that a high through-the-thickness gradient is present. Layerwise models match Pagano's solution and they should be used in the case of local three-dimensional stress state due to localized loadings. As far as failure criteria are concerned, decreasing a/h and for a fixed model, different failure loadings and locations are obtained. The difference is due to the manner each criterion accounts for the out-of-plane stress components. The effect of the stacking sequence has been investigated. It has been

J. Eng. Mech. 2012.138:458-467.

found that the first-ply failure loading strongly depends on the stacking sequence. In particular, for the considered cases, symmetric laminates presents a higher failure loading than unsymmetric ones.

Appendix. Failure Criteria

The failure criteria used in this paper are briefly presented. With the exception of Hashin's criterion, these criteria are of mathematical nature and do not associate a failure mechanism of the composite material.

Maximum Stress Criterion

The maximum stress failure criterion compares the lamina stress status with the material strength parameters:

$$\frac{|\sigma_1|}{X} \geq 1, \qquad \frac{|\sigma_2|}{Y} \geq 1, \qquad \frac{|\sigma_3|}{Z} \geq 1,$$
$$\frac{\sigma_4}{R} \geq 1, \qquad \frac{\sigma_5}{S} \geq 1, \qquad \frac{\sigma_6}{T} \geq 1 \tag{23}$$

$(\sigma_1, \sigma_2, \sigma_3)$ = the normal stress components; and $(\sigma_4, \sigma_5, \sigma_6)$ = shear stress components in the lamina principal coordinates. Normal strengths X, Y, and Z depend on the sign of the corresponding stress component. In the case of tensile stresses, X_T, Y_T, and Z_T should be used in Eq. (23). The compressive strengths X_C, Y_C, and Z_C should be used for compressive normal stresses.

Tsai-Wu's Criterion

In accordance with Tsai-Wu's criterion, Lamina failure occurs when

$$\sum_{i=1}^{3} F_i\sigma_i + \sum_{i=1}^{6} F_{ii}\sigma_i^2 + \sum_{i=1}^{2}\sum_{j=i+1}^{3} F_{ij}\sigma_i\sigma_j \geq 1 \tag{24}$$

The polynomial coefficients are

$$F_1 = \frac{1}{X_T} - \frac{1}{X_C}, \qquad F_2 = \frac{1}{Y_T} - \frac{1}{Y_C}, \qquad F_3 = \frac{1}{Z_T} - \frac{1}{Z_C},$$
$$F_{11} = \frac{1}{X_T X_C}, \qquad F_{22} = \frac{1}{Y_T Y_C}, \qquad F_{33} = \frac{1}{Z_T Z_C}, \qquad F_{44} = \frac{1}{R^2}, \qquad F_{55} = \frac{1}{S^2}, \qquad F_{66} = \frac{1}{T^2}, \tag{25}$$
$$F_{12} = -\frac{1}{\sqrt{X_T X_C Y_T Y_C}}, \qquad F_{13} = -\frac{1}{\sqrt{X_T X_C Z_T Z_C}}, \qquad F_{23} = -\frac{1}{\sqrt{Y_T Y_C Z_T Z_C}}$$

Hoffman's Criterion

Hoffman's failure criterion assumes the same polynomial form as Tsai-Wu's one [see Eq. (24).] The polynomial coefficients are equal to those in Eqs. (25), except for the coupling terms $\{F_{ij}: i \neq j\}$:

$$F_{12} = -\frac{1}{X_T X_C} - \frac{1}{Y_T Y_C} + \frac{1}{Z_T Z_C},$$
$$F_{13} = -\frac{1}{X_T X_C} + \frac{1}{Y_T Y_C} - \frac{1}{Z_T Z_C}, \tag{26}$$
$$F_{23} = \frac{1}{X_T X_C} - \frac{1}{Y_T Y_C} - \frac{1}{Z_T Z_C}$$

Hashin's Criterion

Hashin's failure criterion distinguishes between fiber and matrix failure and between tensile and compressive stress status.

Tensile fiber failure mode, $(\sigma_1 > 0)$:

$$\left(\frac{\sigma_1}{X_T}\right)^2 + \left(\frac{\sigma_5}{S}\right)^2 + \left(\frac{\sigma_6}{T}\right)^2 \geq 1 \tag{27}$$

Compressive fiber failure mode, $(\sigma_1 < 0)$:

$$-\frac{\sigma_1}{X_C} \geq 1 \tag{28}$$

Tensile matrix failure mode, $(\sigma_2 + \sigma_3 > 0)$:

$$\left(\frac{\sigma_2}{Y_T} + \frac{\sigma_3}{Z_T}\right)^2 + \frac{1}{R^2}(\sigma_4^2 - \sigma_2\sigma_3) + \left(\frac{\sigma_5}{S}\right)^2 + \left(\frac{\sigma_6}{T}\right)^2 \geq 1 \tag{29}$$

Compressive matrix failure mode, $(\sigma_2 + \sigma_3 < 0)$:

$$\frac{1}{Y_C}\left[\left(\frac{Y_C}{2R}\right)^2 - 1\right]\sigma_2 + \frac{1}{Z_C}\left[\left(\frac{Z_C}{2R}\right)^2 - 1\right]\sigma_3 + \frac{1}{4R^2}(\sigma_2 + \sigma_3)^2$$
$$+ \frac{1}{R^2}(\sigma_4^2 - \sigma_2\sigma_3) + \left(\frac{\sigma_5}{S}\right)^2 + \left(\frac{\sigma_6}{T}\right)^2 \geq 1 \tag{30}$$

Acknowledgments

First and third authors are partly supported by the Fonds National de la Recherche Luxembourg (FNR) via the CORE project C09/MS/05 FUNCTIONALLY. Second author is supported by FNR through Aides à la Formation Recherche Grant PHD-09-184.

References

Akhras, G., and Li, W. C. (2007). "Progressive failure analysis of thick composite plates using the spline finite strip method." *Compos. Struct.*, 79(1), 34–43.

Basu, S., Waas, A. M., and Ambur, D. R. (2006a). "Compressive failure of fiber composites under multi-axial loading." *J. Mech. Phys. Solids*, 54(3), 611–634.

Basu, S., Waas, A. M., and Ambur, D. R. (2006b). "A macroscopic numerical model for kink banding instabilities in fiber composites." *J. Mech. Mater. Struct.*, 1(6), 979–1000.

Basu, S., Waas, A. M., and Ambur, D. R. (2007). "Prediction of progressive failure in multidirectional composite laminated panels." *Int. J. Solids Struct.*, 44(9), 2648–2676.

Carrera, E. (2003). "Theories and finite elements for multilayered plates and shells: A unified compact formulation with numerical assessment and benchmarking." *Arch. Comput. Methods Eng.*, 10(3), 215–296.
Carrera, E., and Giunta, G. (2009). "Hierarchical evaluation of failure parameters in composite plates." *AIAA J.*, 47(3), 692–702.
Chai, Y., and Gadke, M. (1999). "Impact damage simulation and compression after impact of composite stiffened panels." *Rep. IB 20*, German Aerospace Center (DLR), Cologne, Germany, 99–131.
Chang, K., Liu, S., and Chang, F. (1991). "Damage tolerance of laminated composites containing an open hole and subjected to tensile loadings." *J. Compos. Mater.*, 25(3), 274–301.
Hashin, Z. (1980). "Failure criteria for unidirectional fiber composites." *J. Appl. Mech.*, 47(2), 329–334.
Hill, R. (1948). "A theory of the yielding and plastic flow of anisotropic metals." *Proc.-R. Soc. London, Series A: Math. Phys. Sci.*, 193(1033), 281–297.
Hinton, M. J., and Soden, P. D. (1998). "Predicting failure in composite laminates: The background to the exercise." *Compos. Sci. Technol.*, 58(7), 1001–1010.
Hoffman, O. (1967). "The brittle strength of orthotropic materials." *J. Compos. Mater.*, 1(2), 200–206.
Huang, Z. M. (2001). "Simulation of the mechanical properties of fibrous composites by the bridging micromechanics model." *Composites, Part A*, 32(2), 143–172.
Huang, Z. M. (2007). "Failure analysis of laminated structures by FEM based on non-linear constitutive relationship." *Compos. Struct.*, 77(3), 270–279.
Kam, T. Y., and Jan, T. B. (1995). "First-ply failure analysis of laminated composite plates based on the layerwise linear displacement theory." *Compos. Struct.*, 32(1–4), 583–591.
Kam, T. Y., Sher, H. F., Chao, T. N., and Chang, R. R. (1996). "Predictions of deflection and first-ply failure load of thin laminated composites plates via the finite element approach." *Int. J. Solids Struct.*, 33(3), 375–398.
Kelly, G., and Hallstrom, S. (2005). "Strength and failure mechanism of composite laminates subject to localised transverse loading." *Compos. Struct.*, 69(3), 301–314.
Lee, J. D. (1982). "Three dimensional finite element analysis of damage accumulation in composite laminate." *Comput. Struct.*, 15(3), 335–350.
Mindlin, E. (1951). "Influence of the rotatory inertia and shear in flexural motions of isotropic elastic plates." *J. Appl. Mech.*, 18(1), 31–38.
Mohite, P., and Upadhyay, C. (2006). "Accurate computation of critical local quantities in composite laminated plates under transverse loading." *Comput. Struct.*, 84(10–11), 657–675.
Onkar, A. K., Yadav, D., and Upadhyay, C. S. (2007). "Probabilistic failure of laminated composites plates using the stochastic finite element method." *Compos. Struct.*, 77(1), 79–91.
Padhi, G. S., Shenoi, R. A., Moy, S. S. J., and Hawkins, G. L. (1997). "Progressive failure and ultimate collapse of laminated composite plates in bending." *Compos. Struct.*, 40(3–4), 277–291.
Pagano, N. J. (1970). "Exact solutions for rectangular bidirectional composites and sandwich plates." *J. Compos. Mater.*, 4(1), 20–34.
Pandey, A. K., and Reddy, J. N. (1987). "A post first-ply failure analysis of composites laminates." *28th AIAA/ASME/ASCE/AHS/ASC Structures, Structural Dynamics and Materials Conf.*, American Institute of Aeronautics and Astronautics, Reston, VA, 788–797.
Pinho, S. T., Dávila, C. G., Camanho, P. P., Iannucci, L., and Robinson, P. (2005). "Failure models and criteria for frp under in-plane or three-dimensional stress states including shear non-linearity." *Tech. Rep.*, NASA.
Puck, A. (1996). "Festigkeitsanalyse von faser-matrix-laminaten. Modelle für die praxis." Carl Hanser Verlag München Wien, Munich, Germany (in German).
Puck, A., and Schürmann, H. (1998). "Failure analysis of FRP laminates by means of physically based phenomenological models." *Compos. Sci. Technol.*, 58(7), 1045–1067.
Puck, A., and Schürmann, H. (2002). "Failure analysis of FRP laminates by means of physically based phenomenological models." *Compos. Sci. Technol.*, 62(12-13), 1633–1662.
Reddy, J. N. (2004). *Mechanics of laminated composite plates and shells. Theory and Analysis*, 2nd ed., CRC, Boca Raton, FL.
Reddy, J. N., and Pandey, A. K. (1987). "A first-ply failure analysis of composites laminates." *Comput. Struct.*, 25(3), 371–393.
Reissner, E. (1945). "The effect of transverse shear deformation on the bending of elastic plates." *J. Appl. Mech.*, 12(2), 69–76.
Reissner, E. (1986). "On a mixed variational theorem and on shear deformable plate theory." *Int. J. Numer. Methods Eng.*, 23(2), 193–198.
Sih, G. C., and Skudra, A. M. (1985). *Failure mechanics of composites*, Elsevier Science, New York.
Soden, P. D., Hinton, M. J., and Kaddour, A. S. (1998). "A comparison of the predictive capabilities of current failure theories for composite laminates." *Compos. Sci. Technol.*, 58(7), 1225–1254.
Soni, S. R. (1983). "A new look at commonly used failure theories in composite laminates." *24th Int. Conf. on Structures and Structures Dynamics and Materials*, AIAA/ASME, ASCE/AHS.
Spottswood, S. M., and Palazotto, A. N. (2001). "Progressive failure analysis of a composite shell." *Compos. Struct.*, 53(1), 117–131.
Tsai, S. W., and Wu, E. M. (1971). "A general theory of strength for anisotropic materials." *J. Compos. Mater.*, 5(1), 58–80.
Turvey, G. J. (1980a). "Flexural failure analysis of angle-ply laminates of GFRP and CFRP." *J. Strain Analysis Eng. Des.*, 15(1), 43–49.
Zahari, R., and El-Zafrany, A. (2009). "Progressive failure analysis of composite laminated stiffened plates using the finite strip method." *Compos. Struct.*, 87(1), 63–70.
Zhang, Z., Chena, H., and Yeb, L. (2008). "Progressive failure analysis for advanced grid stiffened composite plates/shells." *Compos. Struct.*, 86(1–3), 45–54.

J. Eng. Mech. 2012.138:458-467.